AD-A126 329 USING SOLAR RADIO BURST INTEGRATED FLUXES TO PREDICT ENERGETIC PROTON FLUX INCREASES(U) AIR FORCE GEOPHYSICS LAB HANSCOM AFB MA W R BARRON 31 AUG 82 1/1

UNCLASSIFIED AFGL-TR-82-0253 F/G 3/2 NL

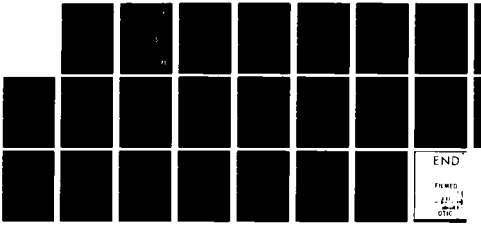

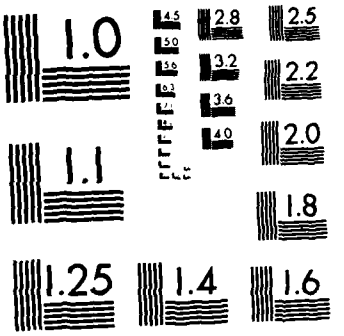

AFGL-TR-82-0253
ENVIRONMENTAL RESEARCH PAPERS, NO. 791

Using Solar Radio Burst Integrated Fluxes to Predict Energetic Proton Flux Increases

WILLIAM R. BARRON

31 August 1982

SPACE PHYSICS DIVISION PROJECT 4643
AIR FORCE GEOPHYSICS LABORATORY
HANSCOM AFB, MASSACHUSETTS 01731

AIR FORCE SYSTEMS COMMAND, USAF

This report has been reviewed by the ESD Public Affairs Office (PA) and is releasable to the National Technical Information Service (NTIS).

This technical report has been reviewed and is approved for publication.

Alva T Stair, Jr.

DR. ALVA T. STAIR, Jr
Chief Scientist

Qualified requestors may obtain additional copies from the Defense Technical Information Center. All others should apply to the National Technical Information Service.

Unclassified

SECURITY CLASSIFICATION OF THIS PAGE (When Data Entered)

REPORT DOCUMENTATION PAGE		READ INSTRUCTIONS BEFORE COMPLETING FORM
1. REPORT NUMBER AFGL-TR-82-0253	2. GOVT ACCESSION NO. AD A124325	3. RECIPIENT'S CATALOG NUMBER
4. TITLE (and Subtitle) USING SOLAR RADIO BURST INTEGRATED FLUXES TO PREDICT ENERGETIC PROTON FLUX INCREASES		5. TYPE OF REPORT & PERIOD COVERED Scientific. Final. 6. PERFORMING ORG. REPORT NUMBER ERP No. 791
7. AUTHOR(s) William R. Barron		8. CONTRACT OR GRANT NUMBER(s)
9. PERFORMING ORGANIZATION NAME AND ADDRESS Air Force Geophysics Laboratory (PHG) Hanscom AFB Massachusetts 01731		10. PROGRAM ELEMENT, PROJECT, TASK AREA & WORK UNIT NUMBERS 62101F 46430306
11. CONTROLLING OFFICE NAME AND ADDRESS Air Force Geophysics Laboratory (PHG) Hanscom AFB Massachusetts 01731		12. REPORT DATE 31 August 1982 13. NUMBER OF PAGES 32
14. MONITORING AGENCY NAME & ADDRESS(if different from Controlling Office)		15. SECURITY CLASS. (of this report) Unclassified 15a. DECLASSIFICATION DOWNGRADING SCHEDULE

16. DISTRIBUTION STATEMENT (of this Report)

Approved for public release; distribution unlimited.

17. DISTRIBUTION STATEMENT (of the abstract entered in Block 20, if different from Report)

18. SUPPLEMENTARY NOTES

19. KEY WORDS (Continue on reverse side if necessary and identify by block number)

Solar flares
Solar radio bursts
Solar protons

20. ABSTRACT (Continue on reverse side if necessary and identify by block number)

Time integrated solar radio fluxes and their association with satellite observed solar energetic proton flux increases have been studied. The time-integration was only of the U-portion of the radio burst flux increase. The best correlations between the integrated radio fluxes and the proton peak fluxes were realized when the radio fluxes were multiplied by the factor $\exp(3B)$, where B is the angular distance, in radians, between the site of the flare and the solar footpoint of the magnetic field connection between the sun

DD FORM 1 JAN 73 1473

Unclassified

SECURITY CLASSIFICATION OF THIS PAGE When Data Entered

20. (Contd)

and the earth. The solar footpoint positions were determined from the solar wind speed.

Two-variate linear regressions were computed using the time-integrated radio fluxes at five discrete radio frequencies in the 606 to 8800 MHz frequency interval and peak proton fluxes at > 10 MeV and > 30 MeV. The higher frequencies of 2695, 4995 and 8800 MHz all correlated better with the > 10-MeV protons than the lower frequencies. The > 30-MeV protons were even better correlated with the higher frequencies, but correlations with the lower frequencies were poorer. The Total Energy Density, E_T, of the radio burst, an integration across the frequency interval of the time-integrated radio fluxes at each frequency, was found to be better correlated with the proton fluxes than any of the individual frequencies.

Three-variate and four-variate linear regressions using different configurations of the time-integrated radio fluxes were also computed. The best of all the correlations was found with the four-variate regression of the three highest frequencies and the > 30-MeV proton flux. Comparisons with other studies have been made, as well as suggestions for use of the results for prediction of PCA and polar D-region phenomena.

Preface

The author wishes to express his thanks to P. Bakshi, J. P. Castelli, E. W. Cliver, D. A. Guidice, S. W. Kahler, M. A. Shea, D. F. Smart, and G. L. Tarnstrom, for many helpful discussions and much generous assistance and guidance during the preparation of this report. Thanks are also extended to K. M. Flaherty for performing the laborious task of typing the document, including its revision and modifications.

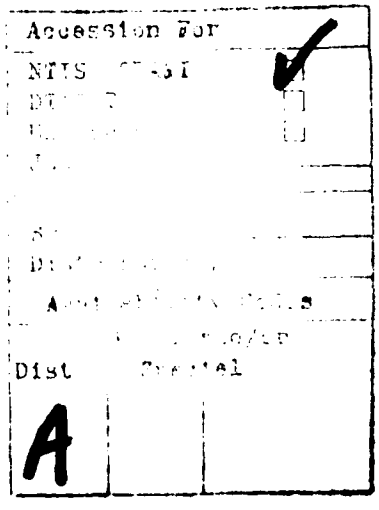

Contents

Illustrations

Illustrations

Tables

Using Solar Radio Burst Integrated Fluxes to Predict Energetic Proton Flux Increases

1. INTRODUCTION

The occurrence of solar flare activity is accompanied by an increase in the flow of energy from the sun into the interplanetary medium. This increased energy flow leaves the sun in the form of various emissions such as radio waves, X-rays, energetic electrons and protons, and alpha particles. The energetic protons, if they reach the earth's environment, make their presence known by increased radio wave absorption in the polar ionosphere. These protons also disturb some human activities; for example, impeding transpolar radio communications [called polar cap absorption (PCA)], lowering the ionospheric D-region height which upsets some radio navigation functions, and disrupting both manned and unmanned space ventures. In some instances the solar flare induced disturbances are of sufficient magnitude to disrupt electric power distribution systems and cause problems in telephone circuits and long distance pipeline distribution systems such as the Trans-Alaska pipeline.[1] These and other disturbances to man's activities have provided an incentive to study the sun, its activity, and the impact of this activity on the terrestrial environment.

(Received for publication 27 August 1982)

1. Carpenter, W.H. et al (1979) Solar-Terrestrial Predictions Proceedings, Vol. II, Working Group Reports and Reviews, International Solar-Terrestrial Predictions Proceedings and Workshop, Boulder, Colorado, 23-27 April 1979.

The purpose of this study has been to find potential relationships between the maximum energetic proton flux, attributable to a solar flare, and the radio emissions from that flare. The effort has been directed to finding adjustments to the peak particle flux, as observed by earth satellites, for the position of the flare on the sun, and combinations of the radio frequencies observed, in order to obtain better possible relationships.

2. BACKGROUND

In relating solar radio burst phenomena to energetic solar particle emissions, Castelli et al[2] and Castelli[3] showed that a particular radio burst peak flux spectrum could be associated with the occurrence of PCA's of 2 dB or larger. The PCA's are related to the increase in the flux of MeV energetic protons.[4-7] The radio spectrum was found to have a U-shape when the peak radio fluxes in the meter through centimeter portions of the radio spectrum were plotted. The time constraint for this condition was that all peaks must occur within a few minutes of each other.[8] The minimum of the U-shaped peak flux spectrum occurs in the decimeter portion of the radio burst spectrum with the peak fluxes rising to $\geq$ 1000 sfu (1 sfu = 1 solar flux unit = 10^{-22} W m^{-2} Hz^{-1}) in the meter and centimeter portions of the radio spectrum. Figure 1 illustrates two U-shaped solar radio burst spectra associated with energetic proton increases observed in the vicinity of the earth.

Several different approaches have been used to find possible ways to relate solar radio burst parameters and energetic particle fluxes. Straka[9] studied radio burst parameters such as burst peak flux, burst mean flux, burst duration and burst-time integrated flux or energy at five frequencies in the 600- to 8800-MHz frequency interval and related them to the peak proton flux of the associated particle event. He found that the time-integrated radio fluxes gave the best correlations with the proton fluxes. He also found that the best correlations were with the lower frequencies in the observation interval even though his sample sizes may have been too small. In this integration of the radio fluxes, Straka[9] integrated the entire flux increase of the burst, including any associated post burst increases. Newell[10] integrated only the start-to-maximum portion of the radio flux increase at the same five radio frequencies. He found that the best correlations between integrated radio fluxes and peak proton fluxes were at the higher frequencies of the frequency band studied. He also found that adjustment of the observed particle flux for the position of the source flare on the face of the sun did not improve the correlation.

(Due to the large number of references cited above, they will not be listed here. See References, page 31.)

Cliver[11] related integrated burst fluxes at 2.8 GHz to PCA magnitudes; he did not find the flare position correction to provide any improvement in the correlation. It is interesting to note that the 2.8-GHz frequency used in the Cliver[11] study falls in the decimeter portion of the radio spectrum; this is the minimum of the U-shaped burst spectral shape found by Castelli et al[2] to be predictive of a proton event having occurred. Akin'yan et al[12] studied both rising portion and the whole burst integrated radio fluxes at frequencies of 3 and 9 GHz. In their study they also made adjustments of the proton fluxes for the heliocentric position of the flare.

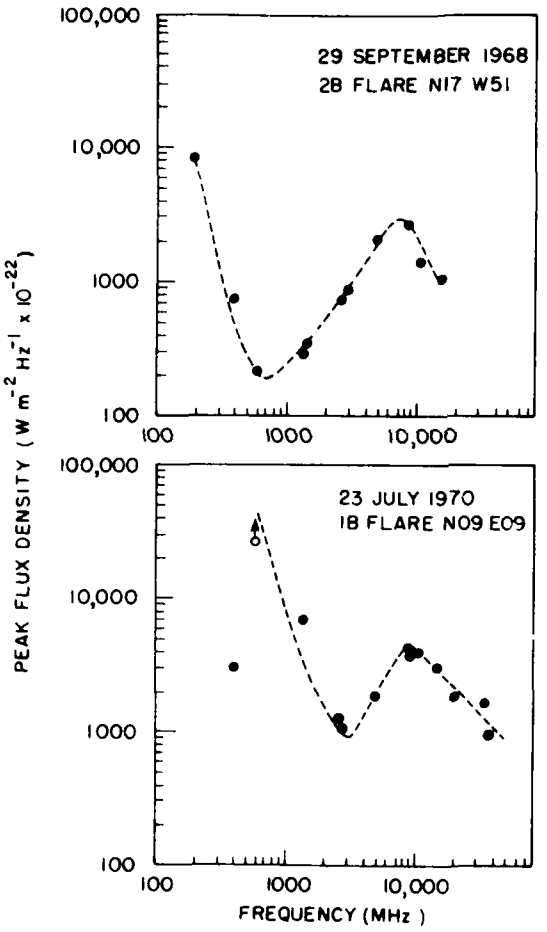

Figure 1. Peak Radio Flux Spectra of Two Solar Proton Flares, Each Showing the U-shaped Spectral Characteristic

11. Cliver, E.W. (1976) Parent-Flare Emission at 2.8 GHz as a Predictor of the Peak Absorption of Polar Cap Events, NELC/TR-2015, Naval Electronics Laboratory Center, San Diego, California 92152.

12. Akin'yan, S.T., Fomichev, V.V., and Chertok, I.M. (1978) Estimates of the intensity of solar protons from the integral parameters of microwave radio bursts, Geomagnet. Aeron. 18(No. 4):395.

All of the studies mentioned here were made at discrete frequencies in the decimeter and centimeter portions of the radio spectrum. Croom[13] also considered several different time and flux characteristics of solar radio bursts such as peak radio flux, mean radio flux, time duration of the burst, and mean duration of the burst as predictors of the peak proton fluxes. He found the mean duration of the burst to be the best predictor. The mean duration of the burst is the time-integrated flux or energy of the burst normalized to its peak flux. One other characteristic of the radio burst to which Croom[13] referred was the total energy density, E_T. A representation of E_T may be found by means of a double integration. First, a time-integration of the radio flux increases is performed at each frequency of observation; then the time-integrated fluxes at the frequencies of observation are integrated across the observed frequency interval to give the total energy density, E_T, of the radio burst

Bakshi and Barron[14] studied the use of E_T as a predictor of > 10 MeV proton flux maxima using integrated fluxes at frequencies of 606, 1415, 2695, 4995 and 8800 MHz. Instead of time-integrating the entire flux increase at each frequency, however, they time-integrated only the portion of the radio burst flux increase that contributed to the U-shape spectrum discussed earlier. In some instances this time-integration was of the entire burst flux increase; in others, it was not. Figures 2 and 3 illustrate the procedure used. Figure 2, an illustration of the solar radio burst observed at the Sagamore Hill Radio Observatory on 28 August 1966, shows an example where only the portion of the burst exhibiting the U-shaped profile in the maximum power spectrum was used to obtain the time-integrated radio fluxes. First, the time-integration of the flux increase at each of the five indicated frequencies was found. At each frequency the trace of the flux increase was broken into a collection (with a small amount of smoothing) of plane triangles, rectangles, and trapezoids (Figure 2). The areas of these plane figures were then found and added together to give the representation of the time-integrated flux for that frequency. The five time-integrated fluxes were then represented, as in Figure 3, to give four trapezoidal figures. The areas of trapezoids enclosed by the adjacent frequencies were found, and finally the four areas were added together to give the E_T for the radio burst being considered. The use of electronic digitizing circuits and computers should make it possible for this process to be more accurately and rapidly performed in the future. These E_T's as well as the time-integrated radio flux at the five frequencies, were then correlated with the peak hourly average > 10 MeV proton flux associated with the radio burst being considered.

13. Croom, D.L., (1971) Forecasting the intensity of solar proton events from the time characteristics of solar microwave bursts, Solar Phys. 19(No. 1):171.

14. Bakshi, P., and Barron, W. (1978) Prediction of the Proton Flux Magnitudes from Radio Burst Data, AFCRL-TR-78-0100, AD A057071.

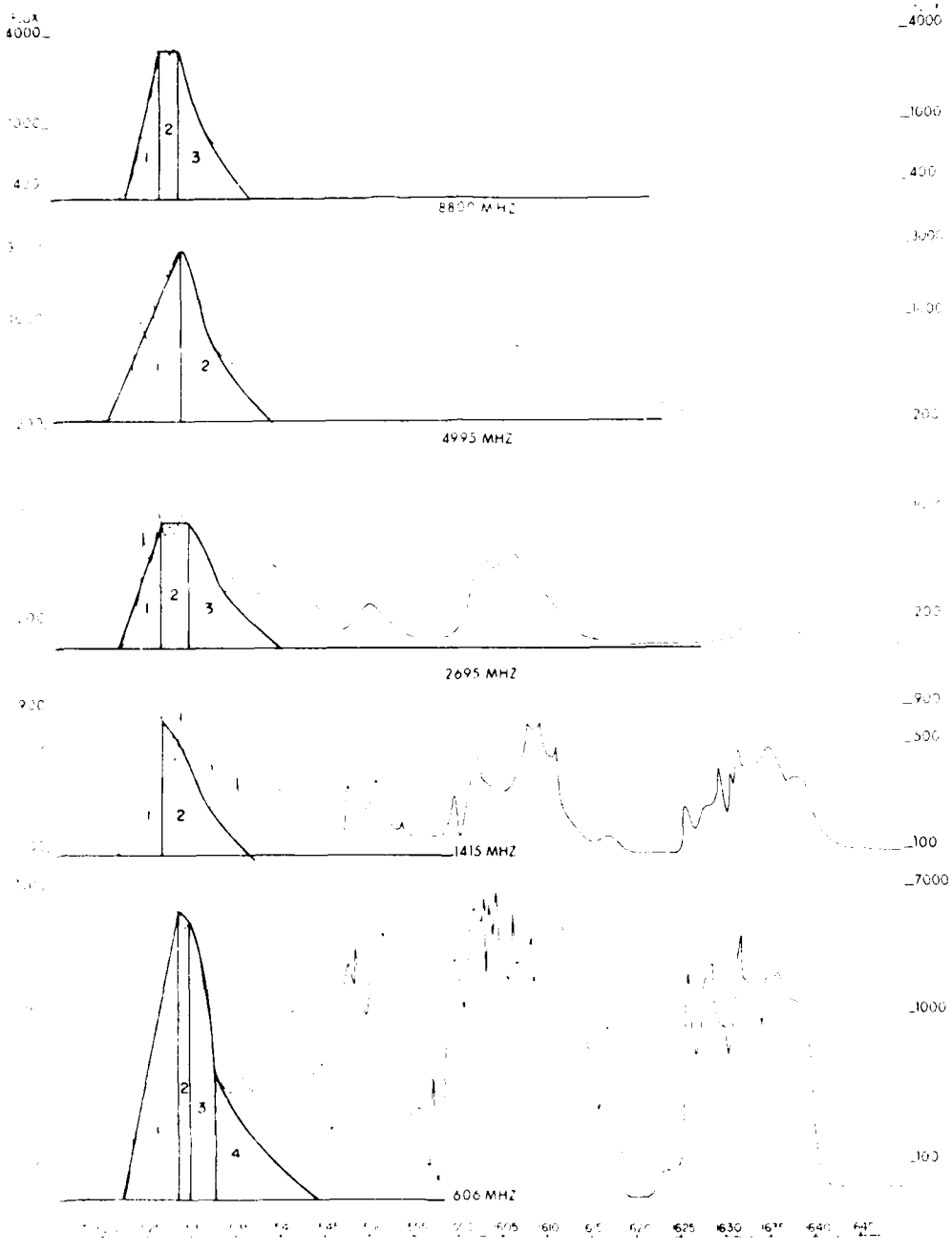

Figure 2. Five Frequency Temporal Radio Flux Variations of 28 August 1966 Solar Proton Flare Observed at the Sagamore Hill Radio Observatory. Only the peak fluxes of the first flux increase exhibited a U-shaped spectrum

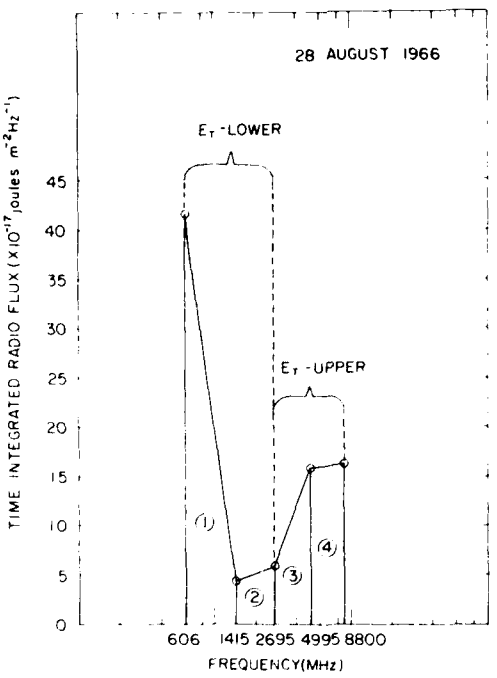

Figure 3. Spectral Representation of Time-Integrated Radio Fluxes of U-Portion of 28 August 1966 Solar Radio Burst

Table 1 gives some of the correlations found. It is seen that, in the case of the integration of individual frequencies, the highest frequencies gave the better correlations. With the exception of 4995-MHz data, the correlations of the individual time-integrated radio fluxes and E_I were further enhanced by the adjustment of the observed peak hourly averaged particle fluxes for the location of the source flare on the face of the sun. The adjustment factor used was e^{3A}, where A is the longitudinal distance, in radians, from the location of the flare to the solar footpoint of the magnetic field lines connecting the earth to the sun at ~ 57° W solar longitude.

Barron and Bakshi[15] found that a better correlation between E_I and the ~ 10-MeV peak particle flux was obtained by using e^{2A} instead of e^{3A}. It has also been found that the e^{2A} adjustment further improves the correlations at the top three individual frequencies in the frequency interval considered, as shown in the last column of Table 1.

It will be the purpose of this report to discuss the effect of adjusting the footpoint position for different solar wind speeds, and different combinations and/or weightings of the time-integrated radio fluxes.

---

15. Barron, W. R., and Bakshi, P. (1979) Application of Integrated Radio Burst Fluxes to the Prediction of Solar Energetic Proton Flux Increases, Solar-Terrestrial Predictions Proceedings, Vol. III: Solar Activity Predictions, International Solar Terrestrial Prediction Proceedings and Workshop, Boulder, Colorado, 23-27 April 1979.

Table 1. Correlation Coefficients

Radio Variables	Proton Variables: Observed I_{10}	Proton Variables: Adjusted for Position $I_{10}e^{3A}$	Proton Variables: Adjusted for Position $I_{10}e^{2A}$
	A		
Time-integrated flux at: (MHz)			
8800	0.718	0.758	0.779
4995	0.781	0.776	0.820
2695	0.759	0.777	0.802
1415	0.601	0.749	0.734
606	0.536	0.707	0.682
	B		
E_T over 606-8800 MHz	0.753	0.806	0.824

3. DATA

The solar radio and energetic particle data used in this study is given in Table 2. These data were obtained from numerous sources such as Solar Geophysical Data (SGD) Reports, Quarterly Bulletins on Solar Activity of the International Astronomical Union, and various observatory reports.

3.1 Radio Data

The radio data are primarily data taken at frequencies of 606, 1415, 2695, 4995, and 8800 MHz at the Sagamore Hill Radio Observatory, the Manila Observatory in the Philippines, and the Athens Observatory in Greece. These observations provided a consistent long-time set of data at the five frequencies mentioned. The peak flux radio burst spectrum of all of the events considered had the U-shaped spectrum described by Castelli et al.[2] In two of the events, 1 and 20, radio data information from observatories other than the three mentioned were used. In event number 1, 24 March 1966, no observations were made at the five indicated frequencies at the time the flare occurred, ~ 0225 UT. In their place the reported values at 500 MHz from Hiraiso Observatory and 1000-, 2000-, 3750-, and 9400-MHz values from Nagoya Observatory in Japan were used. Event 20 was viewed by the Athens Observatory which does not observe at the 606-MHz frequency.

Table 2. Radio and Proton Data, Radio and Solar Wind Data

Radio and Proton Data										
		Optical Flare		Radio Time Integrated Flux $\bar{I}(\omega)$ [a]					Peak Proton Flux [b]	
Index	Date	Type	Location	606 MHz	1415 MHz	2695 MHz	4995 MHz	8800 MHz	I_{10}	I_{30}
1	24 Mar 66	2N	N20W42	(0.27)	(0.33)	(0.75)	(1.55)	(2.14)	(12.24)	(1.94)
2	28 Aug 66	2B	N22E05	41.7	4.20	5.74	15.8	16.2	(13.18)	(3.42)
3	27 Feb 67	2N	N27E02	3.97	3.18	7.68	23.1	45.6	(3.32)	(1.45)
4	23 May 67	3B	N28E28	2175.0	261.0	42.0	75.0	138.0	1036.0	32.15
5	28 May 67	3B	N28W32	3.48	4.65	12.3	10.9	34.8	115.0	26.85
6	29 Sep 68	2B	N17W51	0.39	0.60	2.34	5.19	5.61	31.87	18.89
7	30 Oct 68	3B	S14W37	14.2	4.97	8.76	10.4	7.25	133.87	10.20
8	26 Feb 69	2B	N13W46	17.5	2.20	8.37	9.83	15.6	14.4	5.21
9	27 Feb 69	2B	N13W65	3.42	0.90	4.10	10.6	8.27	28.1	9.31
10	21 Mar 69	2B	N20E17	11.3	2.76	6.17	14.2	15.8	4.74	0.40
11	29 Mar 70	2B	N13W37	0.66	2.75	6.97	19.7	18.8	65.48	20.18
12	23 Jul 70	1B	N09E09	20.7	7.76	1.49	4.46	9.82	11.8	0.8
13	24 Jan 71	3B	N18W49	8.13	7.72	22.3	43.7	50.1	1171.0	408.0
14	06 Apr 71	-B	S19W80	0.23	0.49	2.01	8.49	5.04	51.0	5.0
15	28 May 72	2B	N09E30	6.74	4.12	8.81	10.6	28.8	8.72	2.40
16	04 Aug 72	3B	N14E08	201 6	33.8	62.5	143.6	303.4	68486.0	19773.0
17	07 Aug 72	3B	N14W37	38.9	19.1	37.3	65.1	247.5	3534.0	383.0
18	29 Apr 73	2B	N13W73	7.8	28.5	7.0	12.0	55.0	46.49	12.46
19	12 Oct 77	1B	N07W07	9.90	1.96	1.08	1.28	3.92	(2.86)	(0.66)
20	22 Nov 77	2B	N24W40	(15.21)	4.63	21.30	46.36	51.84	(262.0)	(94.34)
21	07 May 78	2B	N24W68	7.08	3.36	7.23	16.76	27.78	(414.95)	(162.17)

[a] 10^{-17} Joules m^{-2} Hz^{-1}

[b] Protons cm^{-2} sec^{-1} $ster^{-1}$ at > 10 MeV and > 30 MeV

Table 2. Radio and Proton Data, Radio and Solar Wind Data (Contd)

Radio and Solar Wind Data			
Index	Integration of $\bar{T}(\omega)$'s Across the 606-8800-MHz Frequency Internal[c]	$V_{solar\ wind}$[d]	$404/V_{solar\ wind}$
1	10.6	458 (1)	0.88
2	110.6	443 (1)	0.91
3	175.9	414 (1)	0.98
4	1719.0	364 (1)	1.11
5	121.8	640 (1)	0.63
6	31.5	372 (1)	1.09
7	72.2	570 (1)	0.71
8	84.1	470 (1)	0.86
9	57.7	687 (1)	0.59
10	91.9	454 (1)	0.89
11	111.4	457 (1)	0.88
12	51.4	457 (1)	0.88
13	275.8	450 (1)	0.90
14	39.7	488 (1)	0.83
15	110.0	484 (1)	0.83
16	1244.0	804 (2)	0.50
17	825.5	564 (2)	0.72
18	186.6	663 (1)	0.61
19	130.38	385 (3)	1.05
20	298.66	320 (3)	1.26
21	123.33	431 (3)	0.94

a 10^{-16} Joules m^{-2}

b sec^{-1}

(1) Reference: King, (1977)

(2) Reference: King, (1979)

(3) Reference: Solar Geophysical Data

In its place, the radio information at 536 MHz observed at Ondřejov, Czechoslovakia was used. The integrated radio fluxes for all the frequencies of event 1 and the 536-MHz frequency of event 20 were calculated from the event mean flux multiplied by the event duration because the analog traces of these events were not available for integration of the type described earlier. The last three flares in the table, all occurred after the 1976 minimum between solar cycles 20 and 21. Two of those flares, 20 and 21, were observed to occur at 24° N solar latitude, which would make them probable phenomena of cycle 21. Flare 19 was observed at 07° N solar latitude, meaning it was probably a vestigial event of the 20th sunspot cycle.

3.2 Proton Data

The particle data consists primarily of the peak hourly average proton fluxes at > 10 MeV and > 30 MeV as viewed by various Explorer satellites. The first three events and the last three are reconstructed from other energy channels, as > 10 MeV and > 30 MeV channels were not available when these events occurred. The particle flux values used were adjusted by subtraction of background particle flux levels and, when the increase under consideration occurred on top of a prior increase, any flux due to the prior increase was estimated and also removed. One additional possible limitation on the observed proton flux values was pointed out by Croom[13] where he indicated that the true particle flux peak may not be well represented by the hourly average values being reported. When the averaging process is considered, it will be realized that the only instance where the average of a group of values will equal the peak or highest value in the group is when all values in the group are equal to that peak or highest value.

4. CORRELATIONS

Observations of solar flare phenomena by such means as multifrequency radio burst measurements, H-alpha and optical observations, and X-ray measurements all provide information about what is happening in the vicinity of the location of the flare. The radio flux increase measurements give an indication of protons and electrons that have been accelerated at the site of the flare. If this location is a distance from the footpoint of the magnetic field lines connecting the sun and the earth, there is going to be a decrease in the number of flare accelerated particles that will reach the sun-earth magnetic footpoint. There will, therefore, be fewer particles to escape into the interplanetary medium along the field lines to the vicinity of the Earth. Attempts have been made to compensate for this particle loss in various prediction studies, as mentioned earlier.

Van Hollebeke et al[16] noted that the peak 40-MeV particle flux observed by earth satellites appeared to decrease by two orders of magnitude for every radian between the flare site and what they referred to as the "preferred-connection" region. This corresponds to the "optimum longitudinal interval" (OLI) of Akin'yan et al[17] but is not necessarily the "fast propagation region" of Reinhard

16. Van Hollebeke, M. A. I., Ma Sung, L. S., and McDonald, F. B. (1975) The variation of solar proton energy spectra and size distribution with heliolongitude, Solar Phys. 41(No. 1):189.

17. Akin'yan, S. T., Fomichev, V. V., and Chertok, I. M. (1977) Determination of the parameters of solar protons in the neighborhood of the earth from radio bursts: 1. Intensity Function, Geomagnet. Aeron. 17(No. 1):5.

and Wibberenz.[18] With the use of data from Table 2, a comparison was made with the Van Hollebeke et al[16] 10^{2A} coronal gradient attenuation factor to see if some other exponent coefficient would provide a better correlation between the observed > 10-MeV particle flux and the double-integrated radio flux. The adjustment multiplier used with the peak > 10-MeV proton flux was 10^{nA}, where $0 \leq n \leq 2.5$ and A was the solar longitudinal angular distance, in radians, from the location of the flare to the footpoint of the magnetic connection between the sun and the Earth, taken to be at 57° W solar longitude. This is approximately the center of the "preferred-connection" region located in the 20° to 80° W solar longitudinal interval. With A determined for each event, the problem was to find what value of the coefficient n would give the highest correlation between the adjusted > 10-MeV proton peak flux and frequency-time-integrated radio flux, E_T.

The variates correlated were:

X = Log E_T, the independent variable, and

Y = Log $(10^{nA} I_{10})$, the dependent variable.

I_{10} is the peak hourly average > 10-MeV proton flux.

Figure 4 shows the variation of the correlation of Y with X for different values of the coefficient n. The highest value of r, the correlation coefficient, is seen to fall in the interval $1.0 < n < 1.5$. Solution for the maximum of the best fit parabola to the six (n, r) pairs gives $n = 1.274$ and $r = 0.850$. With use of this value of n, the adjusted I_{10} fluxes were calculated and the coefficients of the best fit straight line determined to give

$$Y = 1.845\ X - 1.197$$

where X and Y are as given here. This may also be written as

$$I_{10} \quad (6.5 \times 10^{-2}) 10^{-1.274A} E_T^{1.845}$$

where I_{10} = peak satellite observed > 10-MeV proton flux. Figure 5 illustrates the points from Table 2; the straight line is given by the expression above.

The time-integrated radio fluxes at each of the five frequencies being considered in this study were also correlated with the > 10-MeV proton flux adjusted as mentioned. The results of these correlations and the coefficients of the best-fit straight-line determined from the data set in Table 2 are given in Table 3, along with the

18. Reinhard, R., and Wibberenz, G. (1974) Propagation of flare protons in the solar atmosphere. Solar Phys. 36(No. 2):473.

aforementioned E_T correlations. It is noted that the correlations are higher at the higher three frequencies than at the lower two. In addition, the combination of the time-integrated radio fluxes, E_T, correlates better with the adjusted proton fluxes than do any of the individual frequencies.

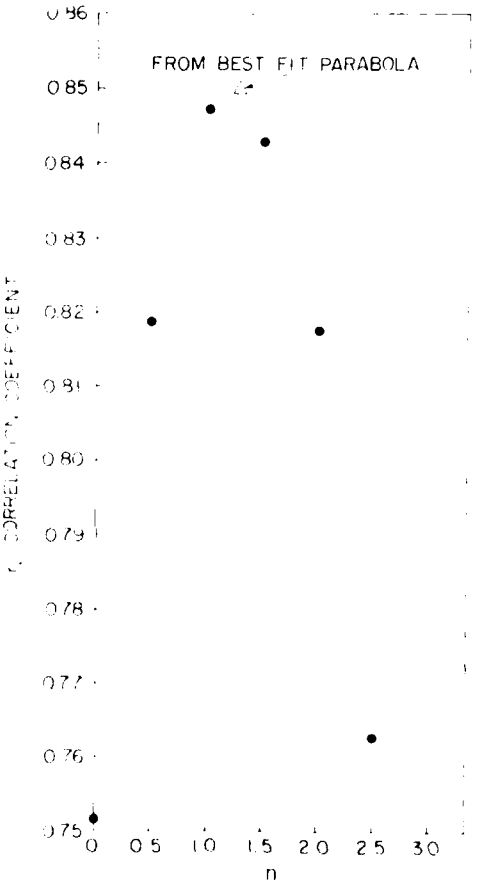

Figure 4. Variations of the Correlation of Log ($10^{nA}I_{10}$) (per Van Hollebeke et al) With Log E_T for Different Values of the Coefficient n. I_{10} is the peak > 10-MeV proton flux; A is the distance, in radians, from the flare site to 57° W solar longitude. The point of maximum correlation is indicated

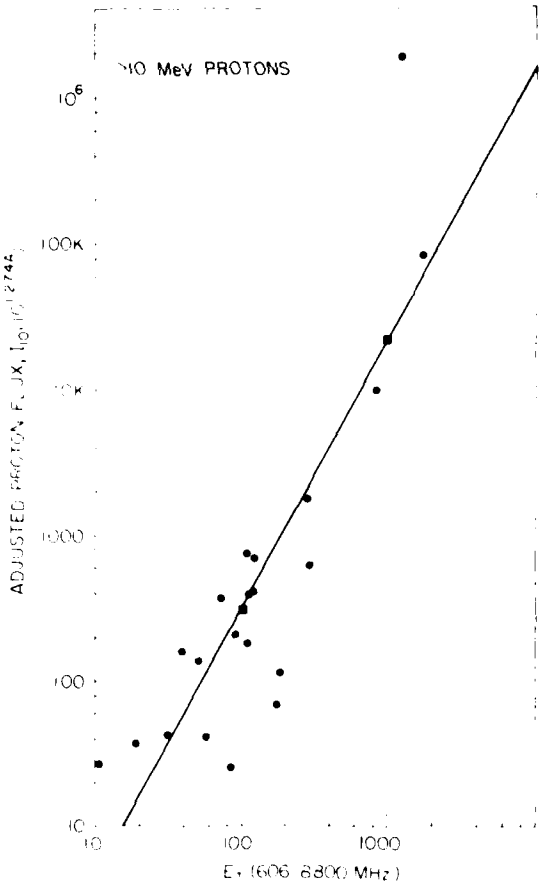

Figure 5. Peak > 10-MeV Proton Fluxes, Multiplied by $10^{1.274A}$, Plotted Against E_T. The straight line best fit to the points is shown

Table 3. Radio and > 10-MeV Proton Correlations (incorporating Van Hollebeke et al [1975] proton flux adjustment)

Frequency (MHz)	Correlation Coefficient r	Straight-line (Y = mX + b) Coefficients b(intercept)	m(slope)
8800	0.804	0.375	1.677
4995	0.806	0.449	1.900
2695	0.803	1.035	1.875
1415	0.753	1.782	1.355
606	0.703	1.806	0.908
606-8800	0.850	-1.197	1.845

4.1 Solar Wind Speed Correction

The discussion thus far has assumed that the footpoint of the magnetic field lines connecting the sun and the Earth was fixed at approximately 57 degrees (1 radian) west of the solar central meridian. In reality, the footpoint of the connecting field lines will vary in position relative to the solar central meridian with changes in the speed of the solar wind.[19] The higher the velocity of the solar wind, the closer to the solar central meridian will be the footpoint of the magnetic field lines which are frozen into the solar wind plasma. The relationship between the solar wind speed V_{SW} in kilometers per second observed at the Earth and the longitudinal position, o_A, in radians, west of the solar central meridian as given by Smart and Shea[20] is:

$$o_A = \frac{404}{V_{SW}} .$$

This expression was used to find the different footpoint positions for the events listed in Table 2. The solar wind speeds used were the closest speeds preceding the time of the solar flare involved, as given by King.[21] The preflare solar wind speed was used because present considerations are for the purpose of predicting the proton flux increase from a solar flare. If the prediction were held up for the changed V_{SW} due to the flare, the energetic particles may already have arrived, making the prediction unnecessary.[22]

The adjustment factor used in this case is e^{nB}, where n is a constant to be determined and B is the angular distance, in radians, between the longitude of the flare and longitude of the footpoint found as described earlier. The procedure was the same as in the previous section: to find the value of n which produced the best correlation, and then the coefficients of the best fit straight line to the data set. Values of n were obtained from correlations of the total energy density, E_T, in the 606 to 8800-MHz frequency interval with adjusted proton fluxes at both > 10-MeV and > 30-MeV energy levels. Figures 6a and 6b show the correlation coefficients obtained for different values of n for the > 10-MeV and > 30-MeV protons, respectively. The values of n for maximum correlation from the two plots are:

n_{10} = 2.682 for > 10-MeV protons,

and

n_{30} = 3.294 for > 30-MeV protons.

(Due to the number of References cited above, they will not be listed here. See References, page 31.)

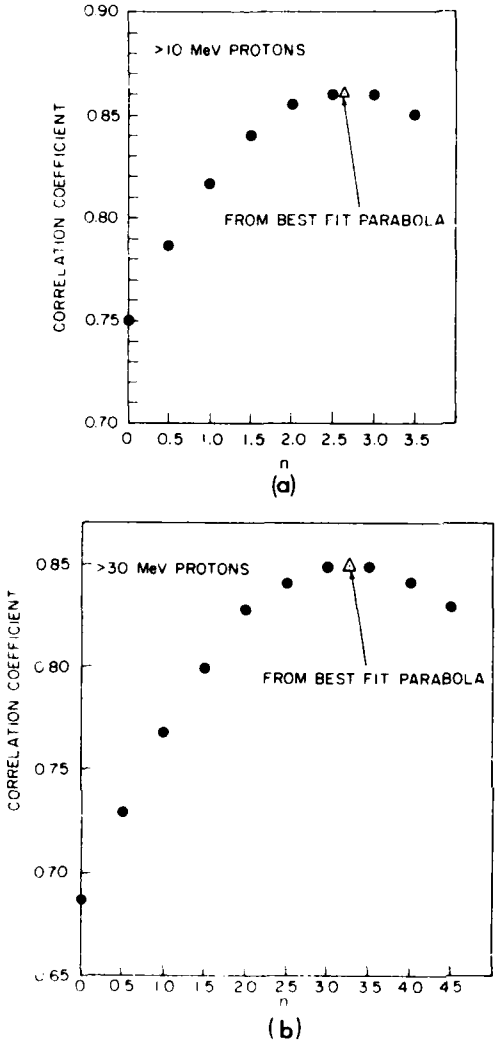

Figure 6. Variation of the Correlation of Log ($e^{nB}I_K$) With Log E_T for Different Values of the Coefficient n. B is the distance, in radians, from the flare site to the solar footpoint of the magnetic Earth-Sun connection as determined from the solar wind velocity. Figure 6a: K = 10, that is, > 10-MeV protons Figure 6b: K = 30, that is > 30-MeV protons. The points of maximum correlation are indicated

By incorporation of these n-values in the e^{nB} adjustment factor, straight-line fits were made to the adjusted proton fluxes and the E_T's of the burst and the five time-integrated radio fluxes. Table 4 gives the results of these straight-line fits. The three higher frequencies are again seen to correlate better than the two lower frequencies. It is also interesting to note that the > 30 MeV correlations are slightly better at the top three frequencies than the > 10 MeV correlations. Plots of the best fit straight lines and the points used to determine them are given in Figure 7 and Figure 8 for > 10 MeV protons and > 30 MeV protons, respectively. The equations of the two straight lines are

> 10 MeV	> 30 MeV
Y = 1.696 X - 0.991, where	Y = 1.642 X - 1.413, where
X = Log E_T (606-8800 MHz) and	X = Log E_T (606-8800 MHz) and
Y = Log $I_{10}e^{2.682\ B}$	Y = Log $I_{30}e^{3.294\ B}$

where B is the solar longitudinal angular distance, in radians, from the location of the flare involved to the magnetic footpoint location as determined from $404/V_{SW}$.

An observation on the results obtained in this consideration is that the value n = 3 used by Smart and Shea,[20] is between the values of n found in this investigation for the > 10 MeV proton fluxes and > 30 MeV proton fluxes; for this reason n = 3 can be used with little degradation of results for the correction factor in both energy channels. It is also a simpler number to use in any computation scheme.

Table 4. Radio and Proton Correlations (magnetic footpoints determined from solar wind speeds)

Frequency (MHz)	Correlation Coefficient r	Straight-line (Y = mX + b) Coefficients b(intercept)	m(slope)
> 10 MeV protons			
8800	0.802	0.490	1.516
4995	0.815	0.529	1.742
2695	0.780	1.125	1.649
1415	0.761	1.688	1.266
606	0.703	1.781	0.823
606-8800	0.861	-0.991	1.696
> 30 MeV protons			
8800	0.825	-0.064	1.529
4995	0.826	0.007	1.730
2695	0.783	0.610	1.625
1415	0.713	1.280	1.140
606	0.646	1.320	0.742
606-8800	0.850	-1.413	1.642

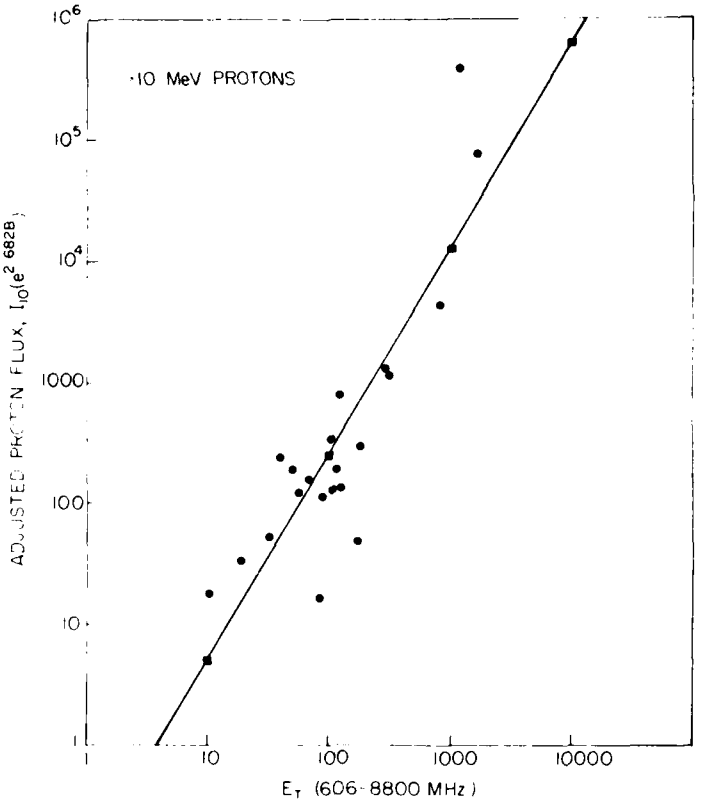

Figure 7. Peak Proton Fluxes, Multiplied by \ppropriate e^{nB}, Plotted Against E_T. The straight line best fit to the points is shown.
> 10 MeV protons

4.2 Multivariate Prediction Study

The results of the correlations performed in the two preceding sections indicated that the best relationship between integrated radio fluxes and adjusted energetic proton fluxes were obtained when the total energy density E_T in the observed frequency band was used.

Results also indicated that in taking the five frequencies involved individually the upper three had better correlations with the proton fluxes. In this section, various multivariate combinations of the integrated fluxes at these frequencies will be made to provide linear fits to the proton data.

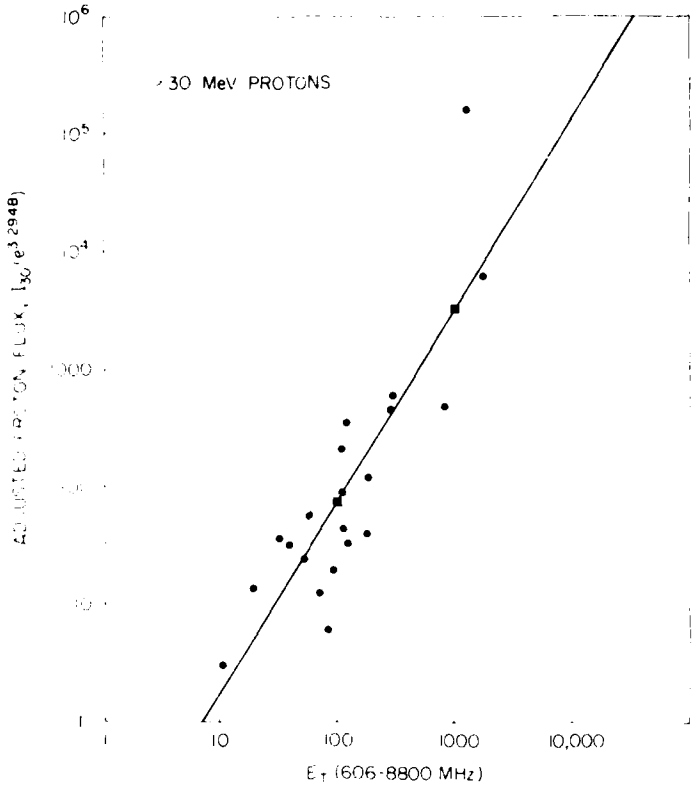

Figure 8. Peak Proton Fluxes, Multiplied by Appropriate e^{nB}, Plotted Against E_T. The straight line best fit to the points is shown. > 30 MeV protons

4.3 Two-variate Linear Regression

Two-variate linear regression is the familiar straight-line fit for finding the coefficients of the expression Y = mX + b. This two-variate linear regression was used in the previous sections employing only time-integrated radio fluxes at discrete frequencies or the total energy density, E_T, as the independent variable and the corrected peak proton flux as the dependent variable. Here we will investigate some different combinations of the time-integrated radio fluxes to provide various independent variables.

In reference to Figure 3, there are four trapezoidal areas indicated, two of which involve the lower three frequencies, and two of which involve the upper three frequencies of the five used in this study. The frequency 2695 MHz is seen to be included in both the upper and lower frequency sets of trapezoids. From Figure 3,

the areas of trapezoids 1 and 2 were combined to give an E_T-lower and the areas of trapezoids 3 and 4 were combined to give an E_T-upper. The E_T-lower and E_T-upper for all the events in Table 2 were then used as the independent variables to obtain the coefficients of the best fit linear regressed expression. Again the fits were made to the logarithms of both the independent and dependent variables. Some fits also were made using the actual values of the data. The results were not very different as far as the correlations between the variates were concerned, but the coefficients obtained were much larger numbers which would be more cumbersome to utilize in a computing scheme. Table 5(a) gives the results of the straight line fits to E_T-lower and E_T-upper with the peak adjusted proton fluxes at > 10 MeV and > 30 MeV energies.

Table 5. Radio and Proton Correlations (various combinations of time-integrated radio fluxes)

(a) Two-Variate Linear Regression, $Y = mX + b$				
	Low Frequency		High Frequency	
	> 10 MeV	> 30 MeV	> 10 MeV	> 30 MeV
r	0.807	0.752	0.826	0.839
b	0.971	0.571	-0.874	-1.397
m	1.322	1.208	1.713	1.707
(b) Three-Variate Linear Regression, $Y = a_0 + a_1 X_1 + a_2 X_2$				
	Low Frequency		High Frequency	
	> 10 MeV	> 30 MeV	> 10 MeV	> 30 MeV
r	0.830	0.792	0.827	0.842
a_0	1.051	0.544	-0.446	-1.065
a_1	-0.029	-0.187	0.447	0.160
a_2	1.650	1.749	1.268	1.530

4.4 Three-variate Linear Regression

Instead of combining the two areas, 1 and 2 for E_T-lower and 3 and 4 for E_T-upper, in Figure 3, a three-variate linear regression fit of the form $Y = a_0 + a_1 X_1 + a_2 X_2$ was performed. The variates in the expression are

Y = Log (adjusted proton flux)

$$X_1 \quad \begin{cases} \text{Log (Trapezoid 1 area from } E_T\text{-lower)} \\ \text{or} \\ \text{Log (Trapezoid 3 area from } E_T\text{-upper} \end{cases}$$

and, respectively,

$$X_2 = \begin{cases} \text{Log (Trapezoid 2 area from } E_T\text{-lower)} \\ \text{or} \\ \text{Log (Trapezoid 4 area from } E_T\text{-upper)} \end{cases}$$

Using the data set in Table 2 to provide the desired variates, we obtained the coefficients given in Table 5(b). Considerations of Table 5(a) and 5(b) show that the three-variate regression gives a better fit to the data set than the two-variate regression. The higher frequencies also are better fit than the lower frequencies, as determined by the correlation coefficients, to the > 30 MeV proton data than to the > 10 MeV proton data.

4.5 Four-variate Linear Regression

The three high frequencies of the five considered, which tend to give better linear regressions to the proton data, were broken apart again to give a four-variate linear regression of the form

$$Y = a_0 + a_1X_1 + a_2X_2 + a_3X_3 ,$$

where

Y Log (adjusted proton flux)

X_1 Log [area of 2695-MHz rectangle, (Figure 9)]

X_2 Log [area of 4995-MHz rectangle, (Figure 9)]

X_3 Log [area of 8800-MHz rectangle, (Figure 9)]

The areas of the three rectangles are found by the product of the time-integrated radio flux at each frequency times the width, in hertz, of the rectangle. This provides a measure of the energy in a frequency band around each frequency of observation. From Figure 9, the width of the rectangles were obtained in the following manner:

The geometric mean frequencies were obtained between each pair of frequencies at which a time-integrated flux was found and the adjacent frequencies above and below it. Call these frequencies the upper mean frequency and the lower mean frequency.

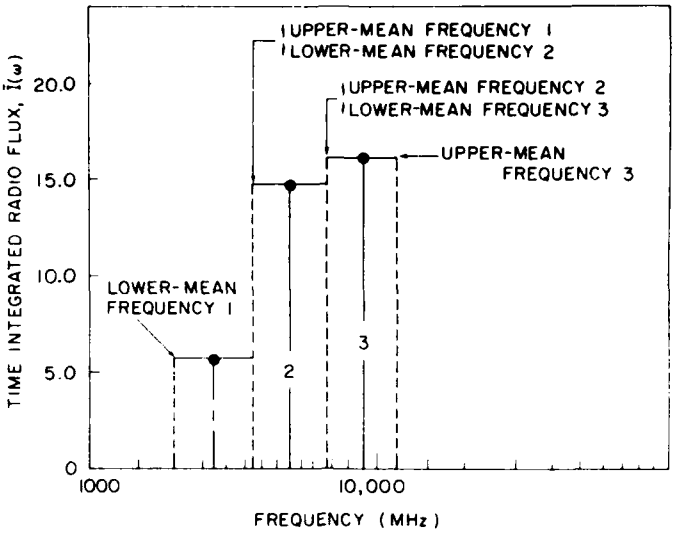

Figure 9. Three-Frequency Spectrum of Time-Integrated Radio Fluxes of U-portion of 28 August 1966 Solar Radio Burst. Associated rectangles used in four-variate linear regression are indicated

The difference between the upper-mean frequency and the lower-mean frequency was then taken as the width of the frequency band around each observed frequency. The upper frequency used to determine the upper-mean frequency for the 8800-MHz area was 15,400 MHz which is the next highest frequency observed at the Sagamore Hill Radio Observatory and the other observatories of the Air Weather Service's Radio Solar Telescope Network (RSTN). The best fit linear regression coefficients were then obtained using the data in Table 2. Table 6 gives the results of this regression. The correlation coefficient, $R_{1,234}$, is called the multiple correlation coefficient of variate 1 on variates 2, 3, and 4. These correspond to Y, X_1, X_2, X_3, respectively, in the expression for the linear fit $Y = a_0 + a_1X_1 + a_1X_2 + a_3X_3$. The quantity $S_{1,234}$ is the standard error of estimate of variate 1 on variates 2, 3, and 4.[23] As would be expected, the correlation coefficient which is a measure of the goodness of the fit of the expression to the data, in each case is the highest one obtained in this study. The >30-MeV proton data are also seen to fit better than the >10 MeV proton data.

23. Spiegal, M. R. (1961) Theory and Problems of Statistics, Schaum's Outline Series, Schaum Pub. Co., New York, N. Y.

Table 6. Radio and Proton Correlations (2695-, 4995-, and 8800-MHz time-integrated radio fluxes)

Four-Variate Regression, $Y = a_0 + a_1 X_1 + a_2 X_2 + a_3 X_3$		
	> 10 MeV	> 30 MeV
$R_{1,234}$	0.870	0.895
$S_{1,234}$	± 0.522	± 0.545
a_0	- 0.789	- 1.523
a_1	- 0.394	- 0.684
a_2	1.293	1.335
a_3	0.808	1.023

5. CONCLUSIONS

Some considerations have been made here of the relationships between the integrated radio fluxes of solar flares and the associated energetic proton flux increases. Adjustments to the particle flux for the position of the flare on the face of the sun have been applied and various combinations and weightings of the integrated radio fluxes have also been tried. In the end, if the correlation coefficient between the variates considered is a measure of their predictive capability, there appear to be several combinations and/or adjustments which are of comparable capability. Just which one will be used will be up to the user and the degree of involvement desired.

Predictions of impending occurrences attempt to foretell what will take place before they actually do and what the magnitude of the occurrences will be. The results of this study may be of use in the following situations:

1. The influx of energetic protons into the polar ionosphere of the earth causes an increased absorption of HF radio signals that pass through the polar ionosphere. This absorption is known as polar cap absorption or PCA. The magnitude of the absorption can be related to the > 10 MeV proton flux by the following expression $P \approx 10A^2$, where P is the proton flux in protons $(cm^2\ sec\ ster)^{-1}$ and A is the 30-MHz riometer absorption in DB.[24] The integrated radio flux, predicting the maximum proton flux increase, will make it possible to determine the absorption to be expected.

24. Castelli, J. P., and Tarnstrom, G. L. (1978) A Catalog of Proton Events 1966-1967, Having Non-Classical Solar Radio Burst Spectra, AFGL-TR-78-0121, AD A060816, Environmental Res. Papers 632, Hanscom AFB, Massachusetts.

2. The increased incidence of energetic protons into the polar ionosphere causes the height of the D-region to be lowered by changing the D-region ionization structure. It has been shown that during a proton flux increase, the height of the south polar D-region tracks the variations in the proton flux reasonably well.[25] Changes in the D-region height influence the propagation of VLF radio signals across the polar caps causing variations in their phase and amplitude structure,[26] which impacts their use for radio navigation purposes. The integrated solar radio flux should make it possible to make an earlier determination of the maximum D-region height change to be expected, from which the disruption of the trans-polar VLF propagation may be anticipated.

3. One requisite of a prediction process is that it provide the prediction as far ahead of its occurrence as possible. Smart and Shea,[27] suggested a method of predicting the end of a proton flux increase by extrapolating the end time of the increase after the maximum of the increase has occurred. The process samples the proton flux levels at a succession of times to obtain the time character of the flux drop-off and then projects the time when the flux increase will be reduced to zero. The same procedure can be applied to the radio flux increase being observed, to predict when the increase returns to zero or to some predetermined level. With that time and the sense of the functional nature of the radio flux decrease, the time-integration of the radio fluxes can be accomplished. With these integrations, the expected peak energetic proton flux can be predicted. This prediction may not be the best possible because the position of the flare on the face of the sun may not be known, but it will at least give a first approximation of the proton flux increase to be expected. For a radio burst of comparatively short duration, the time advantage of the prediction may not be great, but for radio events with longer decay times, and for long duration events of the "nonclassical" type considered by Castelli and Tarnstrom[24] the timeliness of the peak proton flux prediction may be enhanced by as much as an hour or more.

---

25. Helms, W.J. (1978) Polar D-region electron density profiles during a solar proton event, Radio Sci. 13(No. 5):853.

26. Westerlund, S., Reder, F.H., and Åbom, C. (1969) Effects of polar cap absorption events on VLF transmissions, Planet. Space Sci. 17(No. 7):1329.

27. Smart, D.F., and Shea, M.A. (1973) Prediction of the end of solar proton events, Proc. 15th Plenary Meeting of COSPAR, Madrid, Spain, 10-14 May 1972, Space Res. XIII, Vol. 2, Akademie-verlag, Berlin.

References

1. Campbell, W.H. et al (1979) Solar-Terrestrial Predictions Proceedings, Vol. II, Working Group Reports and Reviews, International Solar-Terrestrial Predictions Proceedings and Workshop, Boulder, Colorado, 23-27 April 1979.

2. Castelli, J.P., Aarons, J., and Michael, G. (1967) Flux density measurements of radio bursts of proton producing flares and non-proton flares, J. Geophys. Res., Vol. 72(No. 21);5491; (1969) Radio Burst Spectra and the Short Term Prediction of Solar Proton Events, Proc. of the Symposium of Ionospheric Forecasting, Proc. 49, NATO Advisory Group for Aerospace Res. and Development, Grey Rocks Hotel, St. Jovite, Canada, 2-5 September 1969.

3. Castelli, J.P. (1968) Observation and Forecasting of Solar Proton Events, AFCRL-68-0104, AD 669347.

4. Bailey, D.K. (1964) Polar Cap Absorption, Planet. Space Sci. 12;495.

5. Juday, R.D., and Adams, G.W. (1969) Riometer measurements, solar proton intensities and radiation dose rates, Planet. Space Sci. 17;1313.

6. Potemra, T.A., and Lanzerotti, L.J. (1971) Equatorial and precipitating solar protons in the magnetosphere; 2. Riometer observations, J. Geophys. Res. 76(No. 22);5244.

7. Sellers, B., Hanser, F.A., Stroscio, M.A., and Yates, G.K. (1977) The night and day relationships between polar cap riometer absorption and solar protons, Radio Sci. 12;779.

8. Bakshi, P., and Barron, W. (1979) Prediction of solar flare proton spectral slope from radio burst data, J. Geophys. Res. 84(No. A1);131.

9. Straka, R.M. (1970) The Use of Solar Radio Bursts as Predictors of Proton Event Magnitudes, AFCRL Space Forecasting Res. Note Number 2, June 1970.

10. Newell, D.T. (1972) Forecasting Peak Proton Flux and PCA Event Magnitudes Using Flash-Phase, Integrated Radio Burst Flux Density, AFCRL-72-0543, AD 751925.

References

11. Cliver, E.W. (1976) Parent-Flare Emission at 2.8 Ghz as a Predictor of the Peak Absorption of Polar Cap Events, NELC/TR-2015, Naval Electronics Laboratory Center, San Diego, California 92152.

12. Akin'yan, S.T., Fomichev, V.V., and Chertok, I.M. (1978) Estimates of the intensity of solar protons from the integral parameters of microwave radio bursts, Geomagnet. Aeron. 18(No. 4):395.

13. Croom, D.L. (1971) Forecasting the intensity of solar proton events from the time characteristics of solar microwave bursts, Solar Phys. 19(No. 1):171.

14. Bakshi, P., and Barron, W. (1978) Prediction of the Proton Flux Magnitudes from Radio Burst Data, AFCRL-TR-78-0100, AD A057071.

15. Barron, W.R., and Bakshi, P. (1979) Application of Integrated Radio Burst Fluxes to the Prediction of Solar Energetic Proton Flux Increases, Solar-Terrestrial Predictions Proceedings, Vol. III: Solar Activity Predictions, International Solar-Terrestrial Prediction Proceedings and Workshop, Boulder, Colorado, 23-27 April 1979.

16. Van Hollebeke, M.A.I., Ma Sung, L.S., and McDonald, F.B. (1975) The variation of solar proton energy spectra and size distribution with heliolongitude, Solar Phys. 41(No. 1):189.

17. Akin'yan, S.T., Fomichev, V.V., and Chertok, I.M. (1977) Determination of the parameters of solar protons in the neighborhood of the earth from radio bursts: I. Intensity Function, Geomagnet. Aeron. 17(No. 1):5.

18. Reinhard, K., and Wibberenz, G. (1974) Propagation of flare protons in the solar atmosphere, Solar Phys. 36(No. 2):473.

19. Nolte, J.T., and Roelof, E.C. (1973) Large scale structure of the interplanetary medium, I: High coronal source longitude of the quiet-time solar wind, Solar Phys. 33(No. 1):241.

20. Smart, D.F., and Shea, M.A. (1979) PPS76 - A Computerized "Event Mode," Solar Proton Forecasting Technique, Solar-Terrestrial Predictions Proceedings, Vol. 1, Prediction Group Reports, International Solar-Terrestrial Predictions Proceedings and Workshop, Boulder, Colorado, 23-27 April 1979.

21. King, J.H. (1977) Interplanetary Medium Data Book - Appendix NSSDC/WDC-A-R-S77-04a, National Space Sci. Data Center, National Aeronautics and Space Administration, Goddard Space Flight Center, Greenbelt, Marvland; Interplanetary Medium Data Book, Suppl. 1, 1975-1978, NSSDC/WDC-A-R-S 79-08, Dec. 1979, Nat. Space Sci Data Center, Nat. Aeronautics and Space Admin., Goddard Space Flight Center, Greenbelt, Md.

22. Gosling, J.T. (1976) Transient Phenomena in the Solar Atmosphere and Solar Wind, Physics of Solar Planetary Environment, Vol. 1, Proc. of International Symposium on Solar-Terrestrial Physics, Boulder, Colorado, 17-18 June 1976.

23. Spiegel, M.R. (1961) Theory and Problems of Statistics, Schaum's Outline Series, Schaum Pub. Co., New York, N.Y.

24. Castelli, J.P., and Tarnstrom, G.L. (1978) A Catalog of Proton Events 1966-1967, Having Non-Classical Solar Radio Burst Spectra, AFGL-TR-78-0121, AD A060816, Environmental Res. Papers 632, Hanscom AFB, Massachusetts.

25. Helms, W.J. (1978) Polar D-region electron density profiles during a solar proton event, Radio Sci. 13(No. 5):853.

26. Westerlund, S., Reder, F. H., and Åbom, C. (1969) Effects of polar cap absorption events on VLF transmissions, Planet. Space Sci. 17(No. 7):1329.

27. Smart, D. F., and Shea, M. A. (1973) Prediction of the end of solar proton events, Proc. 15th Plenary Meeting of COSPAR, Madrid, Spain, 10-14 May 1972, Space Res. XIII, Vol. 2, Akademie-verlag, Berlin.

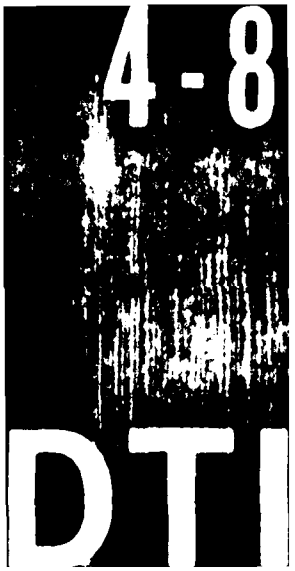
4-8
DTI